TRACKING COMPLEX-VALUED MULTICOMPONENT CHIRP SIGNALS USING A COMPLEX NOTCH FILTER WITH ADAPTIVE BANDWIDTH AND FREQUENCY PARAMETERS

P T Wheeler, J A Chambers

Advanced Signal Processing Group, School of Electronic, Electrical and Systems Eng.
Loughborough University, UK, {p.wheeler2, j.a.chambers}@lboro.ac.uk

ABSTRACT

This paper first demonstrates the ability of a recently developed complex adaptive notch filter (CANF) to track a complex-valued multicomponent chirp signal (CMCS), and provides an analysis of the convergence of the frequency parameter. Next the design is extended, to enable the adaptation of both the frequency and bandwidth parameters; highlighting the need for a steepest ascent approach to adapt the bandwidth parameter. Adapting the notch bandwidth parameter(s) to track a complex sinusoid signal (CSS), or when filters are cascaded for multiple CSSs; allows the design to reduce the noise output from the CANF structure; and this performance advantage is shown in simulations.

Index Terms— adaptive-notch-filter, bandwidth, complex-valued multicomponent chirp signals

1. INTRODUCTION

Many adaptive notch filters (ANFs) have been developed over the last four decades, initially via direct coefficient scaling, and more recently by all-pass forms which are generally considered to provide superior solutions; and in our related research four well known designs were compared in [1]. ANFs have been used in a variety of applications such as: radar, sonar, advanced sensors, and power applications; where some interesting power applications are: active power filters [2], tracking AC phases [3], and removing voltage flicker [4].

In this paper, firstly we demonstrate the ability of the CANF structure due to Wheeler and Chambers [5] to track a CMCS, and we highlight that this design can be directly compared to the structure proposed by Regalia in 2010 [6]. Then we apply an ordinary differential equation approach to confirm the convergence of our frequency estimation algorithm. We note that Regalia's method implements an equation-error approach, whilst we applied an output-error approach which provides a more robust performance as demonstrated in [5].

Then we extend the design to incorporate the ability to adapt the bandwidth parameter of the CANF, and demonstrate the performance improvement achieved when tracking a CMCS and a frequency hopping CSS.

Now to introduce this CANF structure, we begin with the first order z-domain all-pass transfer function

$$A(z) = \frac{z^{-1}\beta - \alpha}{1 - \alpha z^{-1}\beta}. \tag{1}$$

Then by subtracting the output of this transfer function from the input as shown in Fig. 1, a notch function can be created.

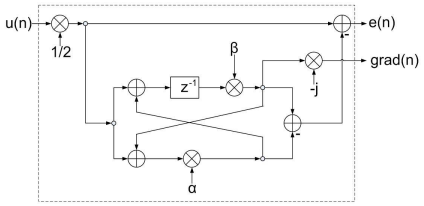

Fig. 1. The CANF proposed in [5], where the structure within the box defined by the dashed line denotes CNF_ in Fig. 5 (b).

The z-domain transfer function for the CANF structure shown in Fig. 1 is derived as $C(z) = \frac{1}{2}\{1 - A(z)\}$, where

$$C(z) = \frac{E(z)}{U(z)} = \frac{1}{2}\frac{(1+\alpha)(1-z^{-1}\beta)}{1-\alpha z^{-1}\beta}. \tag{2}$$

Two parameters may be observed within equation (2), the first of these is $0 \ll \alpha < 1$, which is a real coefficient that controls the notch bandwidth; the second parameter $\beta = e^{j\theta}$, where the value θ is the complex phase shift angle, which is equivalent to the frequency tracked by the CANF.

This paper may be summarised as follows: Section 2 demonstrates the ability of this structure for tracking a CMCS, comparing the performance with Regalia's design [6], then 2.1 analyses convergence of the frequency parameters update. Next, Section 3 discusses the update of the bandwidth parameter, then its update is derived in Section 4; this leads onto results for tracking a CMCS and a hopping CSS in Section 5, and lastly the paper is concluded.

As the topic has been introduced, now tracking CMCSs is investigated.

978-1-4799-2893-4/14/$31.00 ©2014 IEEE

2. TRACKING COMPLEX-VALUED MULTICOMPONENT CHIRP SIGNALS

In Regalia's paper [6], he demonstrated that the complex version of his design is capable of tracking a CMCS, which in this case is a quadratically varying frequency of the form

$$u(n) = A_m e^{j\phi(n)} + b(n); \tag{3}$$

wherein, A_m is a scale factor: which can be taken as real, as if A_m were complex its phase angle would be absorbed into ϕ, leaving behind a real-valued scale factor; $b(n)$ is a white complex circular Gaussian noise process, and $\phi(n)$ is

$$\phi(n) = \phi_2 n^2 + \phi_3 n^3; \tag{4}$$

where the values used to create the CMCS in Fig. 2 are: $\phi_2 = -0.004$ and $\phi_3 = 1.2 \times 10^{-6}$. In [6], Regalia demonstrates the ability of his design to track a CMCS, which we include in this paper as Fig. 2 (a); however, we apply a normalised least mean square (NLMS) update, with an adaptation gain (μ) of 0.08, and γ = 0.8, where γ is the forgetting factor used in the recursive gradient energy estimation.

Equivalently, a comparable result may be produced with the proposed structure, and this result is shown as Fig. 2 (b); which was achieved by using the following parameters: μ = 0.15, γ = 0.8 and α = 0.9 both in Fig. 2 (a) and (b). Note that the learning parameters we used were the optimum settings found empirically to achieve the best tracking performance with minimum variance.

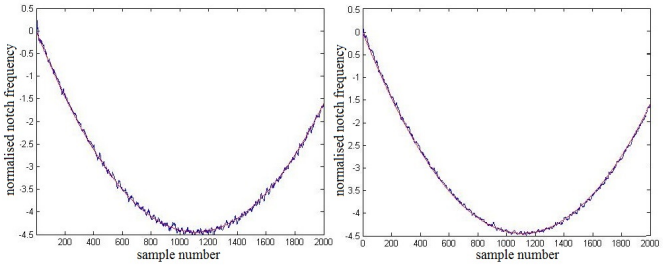

(a) Regalia's approach [6] (b) The proposed structure

Fig. 2. Tracking a complex chirp signal with the two notch filter structures.

Please take note that when tracking a CMCS the variance has been estimated from the 50th to the final sample.

It is clearly visible when comparing Fig. 2 (a) and (b), that the proposed structure produces slightly superior results as compared to Regalia's structure; and this improvement is also clarified by Table 1. Also observe that Table 1 contains a full gradient term for β, which provides a slight improvement; this can be derived in a similar way to the full gradient term for α, which will be shown in Section 4.

Table 1. Comparison of methods for tracking a CMCS.

Method	σ^2
Regalia 2010 [6] - Fig. 2 (a)	0.0026
The proposed structure - Fig. 2 (b)	0.0017
Full gradient for β structure	0.0016

2.1. Convergence of the Frequency Parameter's Update

To demonstrate the convergence of our scheme to the solution, consider the adaptation algorithm applied to a general parameter θ

$$\theta(n+1) = \theta(n) - \mu Re[\frac{e^*(n)grad(n)}{\psi(n)}]; \tag{5}$$

where we are analysing the angle parameter θ, with a fixed α; herein, $grad(n)$ is the gradient shown in Fig. 1, which is calculated as the derivative of the output-error $e(n)$, with respect to θ; and $\psi(n) = \psi(n-1)\gamma + (1-\gamma)(grad(n).grad^*(n))$, noting $(.)^*$ denotes the complex conjugate. Now building upon the approaches in [6] & [11], where [11] shows that for sufficiently slow adaptation, the evolution of the adaptation algorithm is weakly linked to an ordinary differential equation of the form

$$\frac{d\theta}{dt} = E\{Re[\frac{e^*(n)grad(n)}{\Psi}]|\theta\}. \tag{6}$$

Herein as notationally emphasised, the expectation on the right-hand side is evaluated for a fixed θ. Also, to proceed we make the assumption that the normalisation term $\psi(n)$ is a constant, which we denote Ψ.

From (1) the transfer functions $G(z)$ and $F(z)$ linking the input to the notch output and the filter regressor, are given as

$$G(z) = \frac{1+\alpha}{2}\frac{1-e^{j\theta}z^{-1}}{1-\alpha e^{j\theta}z^{-1}} \quad F(z) = \frac{1+\alpha}{2}\frac{-je^{j\theta}z^{-1}}{1-\alpha e^{j\theta}z^{-1}}.$$

Then we may define the expectation $E\{\frac{e^*(n)grad(n)}{\Psi}\}$ as the inner product

$$E\{\frac{e^*(n)x(n)}{\Psi}\} = \frac{1}{2\pi}\int_{-\pi}^{\pi} S_u(\omega)G(e^{j\omega})F^*(e^{j\omega})d\omega; \tag{7}$$

where, $S_u(\omega)$ is the power spectral density of the input defined in (3), which is: $S_u(\omega) = 2\pi A_m^2\delta(\omega-\omega_0)+\sigma^2$, herein ω_0 is the unknown frequency, which gives us the expectation

$$E\{\frac{e^*(n)x(n)}{\Psi}\} = \frac{A_m^2}{\Psi}G(e^{j\omega_0})F^*(e^{j\omega_0}) + \frac{\sigma^2}{2\pi\Psi}\int_{-\pi}^{\pi} G(e^{j\omega})F^*(e^{j\omega})d\omega;$$

wherein,

$$G(e^{j\omega_0})F^*(e^{j\omega_0}) = \frac{(1+\alpha)^2}{4}\frac{(1-e^{j(\omega_0-\theta)})(-je^{-j(\omega_0-\theta)})}{|1-\alpha e^{j(\omega_0-\theta)}|^2}. \tag{8}$$

The real part of this equation then becomes

$$Re(E\{\frac{e^*(n)x(n)}{\Psi}\}) = \frac{A_m^2(1+\alpha)^2}{4\Psi}\frac{\sin(\omega_0-\theta)}{|1-\alpha e^{j(\omega_0-\theta)}|^2}$$
$$+\frac{\sigma^2(1+\alpha)^2}{8\pi\Psi}\underbrace{\int_{-\pi}^{\pi}\frac{\sin(\omega_0-\theta)}{|1-\alpha e^{j(\omega_0-\theta)}|^2}d\omega}_{=0}; \quad (9)$$

herein the noise-induced term vanishes, as this is the integral over one period of a function, which is odd about $\omega_0 = \theta$. Therefore, the associated differential equation becomes

$$\frac{d\theta}{dt} = \frac{A_m^2(1+\alpha)^2}{4\Psi}\frac{\sin(\omega_0-\theta)}{|1-\alpha e^{j(\omega_0-\theta)}|^2}. \quad (10)$$

Then convergence of θ to ω_0 from (10) is shown by choosing a Lyapunov function of the continuous variable t

$$L(t) = [\omega_0 - \theta(t)]^2, \quad \text{to obtain} \quad \frac{dL(t)}{dt}$$
$$= \frac{dL}{d\theta}\frac{d\theta}{dt} = -\frac{A_m^2(1+\alpha)^2}{2\Psi}\frac{(\omega_0-\theta)\sin(\omega_0-\theta)}{|1-\alpha e^{j(\omega_0-\theta)}|^2} < 0,$$

for $\theta \neq \omega_0$.

Now assuming $(\omega_0 - \theta)$ is restricted to the principle range $-\pi \leq \omega_0 - \theta \leq \pi$, which implies that $L(t)$ is monotonically decreasing, so that $\theta(t)$ converges to ω_0 as desired. However, if $|\omega_0 - \theta| > \pi$, then θ converges to $\omega_0 + 2\pi k$: for an appropriate integer k; since θ intervenes through the filter computations purely from the factor $\beta = e^{j\theta(n)}$, a modulo-2π ambiguity in θ is unavoidable.

Next we discuss the method for updating the bandwidth parameter.

3. BANDWIDTH PARAMETER ADAPTATION

Now, to demonstrate the effect of adapting the bandwidth parameter for a frequency hopping CSS, consider Fig. 3.

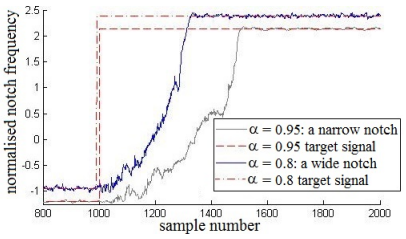

Fig. 3. The effect of utilising different values of α when tracking a CSS.

Observe in Fig. 3 that the 'wide notch' locates the target signal quickly, however has significant noise on the estimate; whilst the 'narrow notch' is slow to locate the target signal but has much less noise on the estimate. Thus, highlighting the benefits of adapting the bandwidth parameter.

Little research has been published to date on updating the bandwidth parameter of any notch filter, although notable references are: [7]-[10]. Unfortunately, these works do not show in detail why a steepest ascent rather than descent approach, is required for adapting the notch bandwidth parameter.

A significant point to note is that when updating the bandwidth parameter (α) a direction of ascent must be applied. This has been implemented previously by other researchers; however, has not been fully explained, which is the case in [8]. To minimise the output mean square error (MSE) the expected result was for α to be adapted with a direction of descent; although, if a steepest descent approach is applied then α converges to minus one.

To provide an explanation for this, if we assume a single CSS input with noise as in [8], whilst β is fixed at the exact correct frequency; then just noise will be output from the CANF. Therefore, the CANF will become as wide as possible to minimise the noise output, thus producing an all-stop response essentially, which does indeed reduce the noise variance.

Now to demonstrate the effect of α increasing observe Fig. 4, where the integral defined in (11) and (12), also clearly increases. Considering this integral implies that a method of steepest ascent should be used to update α, which allows the transfer function to approach the perfect notch case; where the perfect case is when the CSS has been removed, thus leaving purely white noise at the CANF's output.

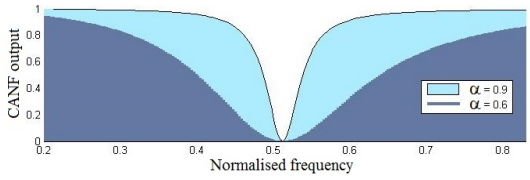

Fig. 4. The magnitude response of the notch filter as a function of two values of the bandwidth parameter.

The equation that defines the noise variance (σ^2) at the CANF output signal is found from the power spectral density, which is

$$\sigma^2 = \frac{1}{2\pi}\int_{-\pi}^{\pi} P(\omega)d\omega; \quad (11)$$

herein $P(\omega)$ is the power spectral density of the CANF output signal. This expression may also be re-arranged as follows

$$\sigma^2 = \frac{\sigma_N^2}{2\pi}\int_{-\pi}^{\pi} |C(\omega)|^2 d\omega, \quad (12)$$

where $C(\omega) = C(z)$ by applying the transformation $z = e^{j\omega}$ as in (2); the last term σ_N^2 is defined as the input noise variance. This implies that a steepest ascent algorithm should be applied in α's update. Thus, the update equation for α is

$$\alpha(n+1) = \alpha(n) + \mu_\alpha Re(e^*(n).grad\_\alpha(n)/\psi_\alpha(n)). \quad (13)$$

Within this equation the term $\psi_\alpha(n)$ is again a recursive calculation of gradient energy, and the gradient of the output MSE with respect to α is $grad\_\alpha(n)$. Note that stability of the CANF is preserved by limiting the maximum value of $\alpha(n)$, and therefore a similar analysis as in Section 2.1 is unnecessary; where $\alpha(n) = \max(0.995, (13))$.

Next we derive an update equation for α, since the correct form of the learning algorithm has been identified.

4. THE UPDATE EQUATION FOR THE BANDWIDTH PARAMETER

To begin the derivation of this full gradient term, recall that the z-domain transfer function for this CANF is

$$C(z) = \frac{E(z)}{U(z)} = \frac{1}{2}\frac{(1+\alpha)(1-z^{-1}\beta)}{(1-\alpha z^{-1}\beta)} = \frac{1}{2}(1+\alpha)(1-z^{-1}\beta)(1-\alpha z^{-1}\beta)^{-1}. \quad (14)$$

Then differentiating the products containing α, yields the equation for the update of α to be

$$\frac{GRAD\_\alpha(z)}{U(z)} = \frac{1}{2}[\frac{(1+z^{-1}\beta)}{(1-\alpha z^{-1}\beta)} \times \frac{(1-z^{-1}\beta)}{(1-\alpha z^{-1}\beta)}], \quad (15)$$

where a second filter is required to implement this expression; and (15), can be implemented as shown in Fig. 5 (a).

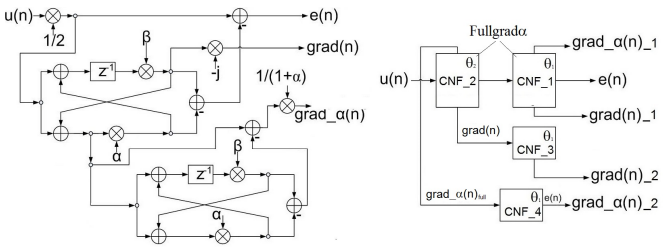

(a) A structure that can apply α's update, for tracking one CSS.

(b) The structure required for tracking two CSSs, whilst adapting individual α values.

Fig. 5. Structures capable of implementing α's update for tracking one and two CSSs.

Then, the complete structure necessary for tracking two CSSs is shown in Fig. 5 (b). Table 2 now shows the additional complexity required to adapt α.

Tracking a single CSS				Tracking two CSSs		
Method	÷s	×s	+s	÷s	×s	+s
The Orig. appr.	2	10	8	4	24	21
Adapting α	4	19	15	8	43	42

Table 2. The computational complexity for tracking one and two CSSs, with α fixed then adapting, at one time sample.

Moving on, the next section of this paper contains the result for tracking a CMCS and a frequency hopping CSS.

5. TRACKING A CMCS AND A FREQUENCY HOPPING CSS

This section contains the results for tracking a CMCS and a frequency hopping CSS simultaneously. Firstly, with a fixed value of α; then α is adapted: which is shown in Table 3.

	CMCS_1		CMCS_2	
Method	σ_1^2	σ_2^2	σ_1^2	σ_2^2
$\alpha = 0.8$	7.02e-04	5.76e-04	7.75e-04	8.17e-04
Adapt. α	8.96e-06	6.45e-05	3.13e-05	1.62e-04

Table 3. Comparison of the variances with a fixed then adapting α values, whilst tracking a chirp and a hopping CSS.
Wherein, for CMCS_1: $\phi(n) = 0.1 \times 10^{-6}n^3 - 0.0005n^2$
and for CMCS_2: $\phi(n) = 0.3 \times 10^{-6}n^3 - 0.002n^2 + 2n$.

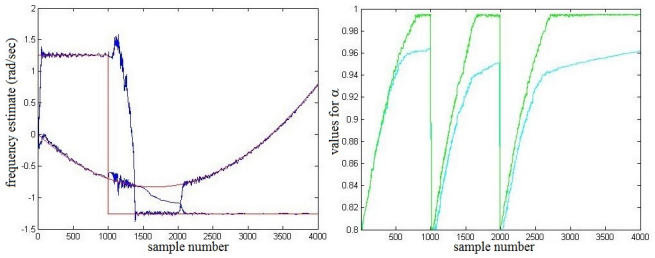

a) The adaptation of both α values in this CANF.

b) The tracking performance of the CANF.

Fig. 6. Tracking a CMCS and a hopping CSS simultaneously, whilst adapting values of α for each signal. Herein: $\mu_\beta = 0.1$, $\mu_\alpha = 0.001$, $\gamma_\beta = 0.9$ and $\gamma_\alpha = 0.8$.

Table 3 and Fig. 6 demonstrate that adapting α generates a significant improvement to both signals.

Please note, the improvement gained from adapting the α whilst tracking frequency hopping CSSs with this approach, will be published in [12].

6. CONCLUSION

This paper demonstrated the strong performance of a new CANF for tracking a CMCS, as compared to [6].

We also showed that a method of steepest ascent is required for the adaptation of the bandwidth parameter α; and demonstrated that the performance of the CANF can be significantly improved if both the bandwidth and frequency parameters are updated simultaneously when tracking a hopping CSS and a CMCS.

The computational complexities with and without the adaptation of α have been included in this paper; this demonstrated that although the performance of this CANF structure can be significantly improved by adapting the bandwidth parameter, this may double the complexity of the design: which may be significant in real-time processing.

7. REFERENCES

[1] P. T. Wheeler, J. A. Chambers. "Real Adaptive Notch Filter Analysis and a New Structure Developed for Tracking Complex Sinusoidal Signals", in the 9th IMA International Conference on Mathematics in Signal Processing, Dec. 17-20 2012.

[2] R. R. Pereira, C. H. da Silva, L. E. B. da Silva, G. Lambert-Torres, J. O. P. Pinto. "New Strategies for Application of Adaptive Filters in Active Power Filters", Industry Applications, IEEE Transactions on , vol.47, no.3, pp. 1136–1141, May-June 2011.

[3] M. Karimi-Ghartemani. "A novel three-phase magnitude-phase-locked loop system", Circuits and Systems I: Regular Papers, IEEE Transactions on , vol.53, no.8, pp. 1792–1802, Aug. 2006.

[4] A. El-Nady, A. Noureldin. "Mitigation of Arc Furnace Voltage Flicker Using an Innovative Scheme of Adaptive Notch Filters", Power Delivery, IEEE Transactions on , vol.26, no.3, pp. 1326–1336, July 2011.

[5] P. T. Wheeler, J. A. Chambers. "Complex adaptive notch filter structure for tracking multiple complex sinusoidal signals", Electronics Letters, vol.49, no.3, pp. 179–181, Jan. 2013.

[6] P. A. Regalia. "A Complex Adaptive Notch Filter", Signal Proc. Letters, IEEE, vol. 17, pp. 937–940, Nov. 2010.

[7] K. M. Knill, A. G. Constantinides. "Least-mean square adaptation of the orthogonal block adaptive line enhancer", Signals, Systems and Computers, 1993 Conference Record of the Twenty-Seventh Asilomar Conference, pp. 663–667, vol.1, Nov. 1993.

[8] A. Mvuma, S. Nishimura, T. Hinamoto. "Adaptive optimization of notch bandwidth of an IIR filter used to suppress narrow-band interference", Circuits and Systems, ISCAS 2002. in the IEEE International Symposium on , pp. V-341–V-344 vol.5, May 2002.

[9] R. Punchalard, W. Lertvasana, P. Chumchu. "Convergence speed improvement for a variable step-size plain gradient algorithm by using variable notch bandwidth technique", Image and Signal Processing and Analysis, ISPA 2003. in the 3rd International Symposium on , pp. 788–792 vol.2, Sept. 2003.

[10] J. Levin, P. Ioannou. "Multirate adaptive notch filter with an adaptive bandwidth controller for disk drives", American Control Conference, 2008, pp. 4407–4412, June 2008.

[11] Ljung, L., "Analysis of recursive stochastic algorithms", Automatic Control, IEEE Transactions on , vol.22, no.4, pp. 551–575, Aug. 1977.

[12] P. T. Wheeler, J. A. Chambers. "Simultaneous Adaptation of Bandwidth and Frequency Parameters within a Complex Notch Filter", to appear in the Intelligent Signal Processing Conference, London, Dec. 2013.